

[View the Full Text HTML](#)



Zn(tbip) ($\text{H}_2\text{tbip} = 5\text{-tert-Butyl Isophthalic Acid}$): A Highly Stable Guest-Free Microporous Metal Organic Framework with Unique Gas Separation Capability

Long Pan, Brett Parker, Xiaoying Huang, David H. Olson, JeongYong Lee, and Jing Li*

Department of Chemistry and Chemical Biology, Rutgers University, 610 Taylor Road, Piscataway, New Jersey 08854

Received November 21, 2005; E-mail: jingli@rutchem.rutgers.edu

Recent studies have uncovered numerous interesting and promising gas sorption properties of microporous metal organic frameworks (MMOFs), including gas separation¹ and hydrogen sorption.² However, for any practical applications, it is very important that these MMOF materials are structurally robust and thermally stable. Unfortunately, thermal instability is a major problem for many of the MMOFs. Even at reasonably modest temperatures, very few of those containing guest molecules can survive extended heating. The removal of the guest molecules drastically reduces their stability and likelihood for commercial applications. Guest-free metal organic frameworks (GFMMOFs) generally have significantly higher thermal stability. In addition, because the pore dimensions of the GFMMOFs typically fall in the range of ultramicropores ($<7 \text{ \AA}$),^{2g} they often exhibit a high adsorption selectivity that is particularly attractive for separation of small gas molecules. The small pore diameters are also desirable for storing hydrogen. $[\text{Cu}(\text{hfipbb})] \cdot (\text{H}_2\text{hfipbb})_{0.5}$ [$\text{H}_2\text{hfipbb} = 4,4'$ -(hexafluoroisopropyl idene)bis-(benzoic acid)], for example, is a GFMMOF that has shown very interesting gas sorption properties.^{1c,2b} It demonstrates an unusually high structural and thermal stability, and its crystal structure remains intact upon repeated heating at $330 \text{ }^\circ\text{C}$. Here we report a new GFMMOF, Zn(tbip) (**1**) (tbip = 5-*tert*-butyl isophthalate). Remarkably, it possesses a unique capability for separation of dimethyl ether (DME) from methanol (MeOH) and MeOH from water.

Single crystals of **1** were grown hydrothermally.³ We selected H_2tbip as the ligand, in view of its bulky aliphatic groups, to attempt to build hydrophobic and solvent-free channel frameworks using water as a solvent. Its crystal structure was determined by single-crystal X-ray diffraction.⁴ Tetrahedral zinc centers are linked by tbip ligands to generate a three-dimensional framework. Each tetrahedral Zn(II) cation occupies a 2-fold rotation symmetry position. All adjacent zinc nodes are bridged, along the *c* axis, by two carboxylic groups to form a 3_1 helical chain with a pitch of 7.977 \AA along the crystallographic *c* axis (screw axis). The shortest zinc–zinc intrachain distance is 3.38 \AA . Each chain connects to three identical neighboring chains through tbip, giving rise to the closest interchain distance of 7.212 \AA . This results in a 3D structure containing close-packed 1D open channels (or microtubes) along the *c* direction. The diameter of these channels is sufficiently small that they are highly stable without guest molecules (Figure 1). With a 3.55 \AA (tile) and 3.25 \AA (perpendicular) distance between the phenyl rings that form the channel walls, strong π – π interactions via a slipped π stacking mode are anticipated.⁵ Note these distances are comparable with the value in graphite (3.35 \AA).

All three methyl groups of the ligand are disordered and protrude into the channels. Measurement of the shortest distance of hydrogen atoms of two opposite butyl groups gives the narrow window of 4.5 \AA (excluding the van der Waals radius of hydrogen). The aperture of the channels in **1** is on the same order as the cross-

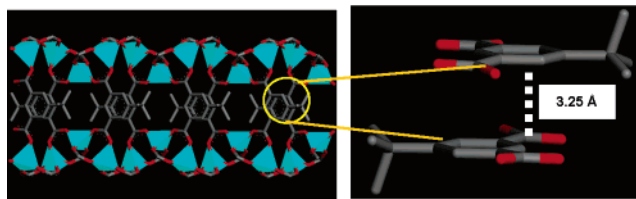
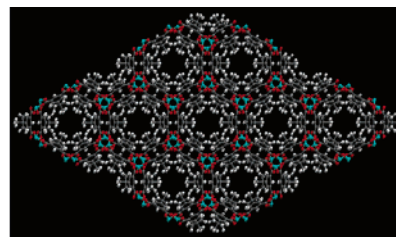


Figure 1. Top: Crystal structure of Zn(tbip) (**1**) showing close-packed channels. Bottom left: The channel wall; ZnO_4 polyhedron. Bottom right: Phenyl rings with strong π – π interaction.

section of $[\text{Cu}(\text{hfipbb})] \cdot (\text{H}_2\text{hfipbb})_{0.5}$,^{1c,2b} but the free accessible volume of 17.7% calculated from PLATON⁶ is significantly higher, as a result of more effective packing of the channels.

There has been some concern on practical utility of porous metal organic materials due to their thermal instability. Many of these compounds being investigated are incapable of withstanding prolonged and repeated heating, even at relatively mild temperatures. However, as an exception, GFMMOFs can possess exceptionally high thermal stability. Thermogravimetric (TG) analysis of **1** showed that no weight loss occurred during a prolonged heating at $350 \text{ }^\circ\text{C}$ (over 24 h).⁷ The structure retained its crystallinity fully. This was verified by PXRD analysis immediately after TGA. This remarkable feature demonstrates that MMOFs of this type may indeed be suitable for applications that require frequent adsorption–desorption cycles over long time periods, such as on-board hydrogen storage.

The pore characteristics and hydrogen adsorption capabilities of **1** were characterized by gas sorption study using a previously described procedure.^{2f,g} The DA (Dubinin–Astakhov)^{2a} pore volume of **1** was calculated to be 0.14 and $0.15 \text{ cm}^3/\text{g}$ based on the N_2 and Ar sorption data collected at 77 and 87 K , respectively (Figure 2a). Both follow a typical Type I isotherm. A gravimetric density of 0.75 and $0.52 \text{ wt } \%$ of hydrogen was achieved at 77 and 87 K and 1 atm , respectively (Figure 2b). The density of adsorbed H_2 at 77 K and 1 atm , calculated to be $0.054 \text{ g}/\text{cm}^3$, is as high as that of our previously reported value,^{2f} $0.053 \text{ g}/\text{cm}^3$, which is one of the highest values among the porous metal organic frameworks reported to date. This high hydrogen density was achieved with relatively small multipoint BET surface area, $256 \text{ m}^2/\text{g}$, from N_2

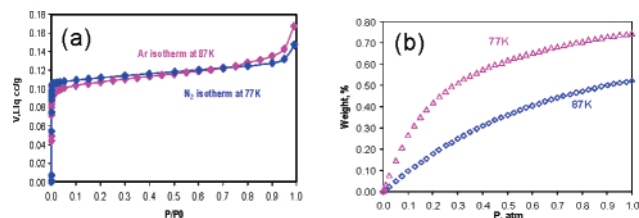


Figure 2. Adsorption isotherms for **1**: (a) Ar (87 K) and N₂ (77 K); (b) N₂ (77 and 87 K).

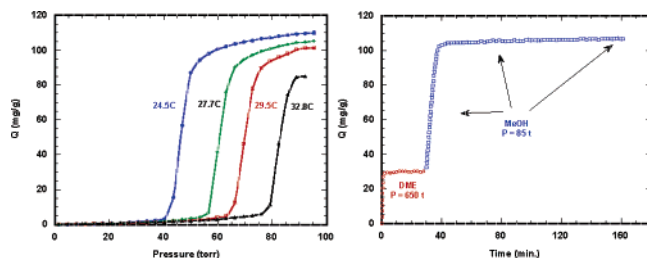


Figure 3. Left: MeOH adsorption isotherms at different temperatures. Right: Adsorption of DME at 30 °C followed by MeOH on **1**.

adsorption data at 77 K, and smaller pores compared to [M₃(bpdC)₃-bpy]·4DMF·H₂O (M = Co or Zn).^{2e,f} In addition, the isosteric heats of hydrogen adsorption Q_{st} of **1** were calculated to be 6.7–6.4 kJ/mol (coverage 0.02–0.5 wt %). These values are similar to those of [Co₃(bpdC)₃bpy]·4DMF·H₂O,^{2f} suggesting a relatively strong adsorbent–adsorbate interaction. It leads us to believe this high density is a result of suitable pore diameter (comparable to H₂ kinetic diameter) and effective pore structure (close-packed 1D channels).

The new MMOF material is also of great interest because of its potential for unique applications in gas separation. The effective cross-section of the 1D channels in **1** is ~4.5 Å, allowing it to adsorb normal paraffins, methanol (MeOH), and dimethyl ether (DME) but to exclude aromatics. The intimate relationship between MeOH and DME in important reactions such methanol to olefins and methanol to gasoline made them prime candidates for our gas sorption study. Compound **1** has the property of being very hydrophobic, exhibiting essentially zero water adsorption (<~1 mg/g at $P/P^0 = 0.65$) but adsorbing high volumes of methanol, 110 mg/g at 24.5 °C and 90 Torr MeOH ($P/P^0 = 0.73$). The shape of the MeOH adsorption isotherms (Figure 3) is typical for an adsorbent that exhibits relatively weak interactions with the adsorbate, adsorbing less than ~3 mg/g up to 40 Torr followed by a very sharp increase in adsorption as capillary condensation fills the pores with MeOH. The condensation point shifts ~4.7 Torr/1 °C, indicating that at ~15 °C capillary condensation should occur at very low pressure (e.g. 1 Torr MeOH). The Zn(tbip)/MeOH system also exhibits hysteresis (Supporting Information). The adsorption properties of **1** may be compared with those of pure silica ZSM-5 (4 ppm Al, silicalite), which is hydrophobic but adsorbs as much as 7 mg/g of water at $P/P^0 = 0.65$ and shows moderate affinity for MeOH (Supporting Information). Its MeOH adsorption isotherms are fitted reasonably by the Langmuir equation, with adsorption beginning at low pressures but not exhibiting the sharp increase associated with capillary condensation.

Zn(tbip) also exhibits potential for the separation of DME from MeOH. The adsorption of DME, followed by MeOH, is illustrated in Figure 3. At 30 °C, 650 Torr ($P/P^0 = 0.13$), 30 mg/g of DME is rapidly adsorbed on **1**. After 30 min, simultaneously, the pressure of DME is set to zero and MeOH is introduced at 85 Torr. As DME desorbs ($P = 0$) it is replaced by MeOH and quickly reaches

the 105 mg/g adsorption level. Several separation schemes are possible. For example, at conditions of T and P below the MeOH capillary condensation point, DME will selectively adsorb for facile separation from MeOH. In a second case, T is chosen to maximize the difference between DME and MeOH adsorption, and after adsorption of the binary gases, a few degrees increase in temperature will result in desorption of a majority of the MeOH and a relatively small amount of DME. The isosteric heat of adsorption of DME computed from adsorption isotherms (Supporting Information), at $Q = 10$ mg/g loading, is 51 kJ/mol and is similar to that of MeOH ($Q = 60$ mg/g loading points of Figure 3), 53 kJ/mol. Note the latter heats include substantial adsorbate–adsorbate contributions.

Acknowledgment. Partial support from the donors of the Petroleum Research Fund administered by the ACS (PRF #42614-AC3,10) and from the National Science Foundation (DMR-0422932) is gratefully acknowledged.

Note Added after ASAP Publication: In the version published on the Internet March 14, 2006, the Supporting Information was incomplete. The version of SI published March 16, 2006 is complete.

Supporting Information Available: Tables of atomic coordinates of all atoms, isotropic and anisotropic thermal parameters, bond distances and angles, crystallographic data for the compound (PDF). This material is available free of charge via the Internet at <http://pubs.acs.org>.

References

- (1) (a) Pan, L.; Adams, K. M.; Hernandez, H. E.; Wang, X.; Zheng C.; Hattori, Y.; Kaneko, K. *J. Am. Chem. Soc.* **2003**, *125*, 3063. (b) Matsuda, R.; Kitaura, R.; Kitagawa, S.; Kubota, Y.; Belosludov, R. V.; Kobayashi, R. C.; Sakamoto, H.; Chiba, T.; Takata, M.; Kawazoe, Y.; Mita, Y. *Nature* **2005**, *436*, 238. (c) Pan, L.; Olson, D. H.; Ciemmolonski, L. R.; Heddy, R.; Huang, X.-Y.; Li, J. *Angew. Chem., Int. Ed.* **2006**, *45*, 616.
- (2) (a) Rosi, N. L.; Eckert, J.; Eddaoudi, M.; Vodak, D. T.; Kim, J.; O’Keeffe, M.; Yaghi, O. M. *Science* **2003**, *300*, 1127. (b) Pan, L.; Sander, M. B.; Huang, X.-Y.; Li, J.; Smith, M.; Bittner, E.; Bockrath, B.; Johnson, J. A. *J. Am. Chem. Soc.* **2004**, *126*, 1308. (c) Rowsell, J. L. C.; Millward, A. R.; Park, K. S.; Yaghi, O. M. *J. Am. Chem. Soc.* **2004**, *126*, 5666. (d) Dincă, M.; Long, J. R. *J. Am. Chem. Soc.* **2005**, *127*, 9376. (e) Kesani, B.; Cui, Y.; Smith, M. R.; Bittner, E. W.; Bockrath, B. C.; Lin, W. B. *Angew. Chem.* **2005**, *44*, 72. (f) Lee, J.-Y.; Pan, L.; Kelly, S. K.; Jagiello, J.; Emge, T. J.; Li, J. *Adv. Mater.* **2005**, *17*, 2703. (g) Lee, J.-Y.; Jagiello, J.; Li, J. *J. Solid State Chem.* **2005**, *178*, 2572. (h) Rowsell, J. L. C.; Yaghi, O. M. *Angew. Chem., Int. Ed.* **2005**, *44*, 4670. (i) Zhao, X.; Xiao, B.; Fletcher, A. J.; Thomas, K. M.; Bradshaw, D.; Rosseinsky, M. J. *Science* **2004**, *306*, 1012. (j) Lee, E. Y.; Jang, S. Y.; Suh, M. P. *J. Am. Chem. Soc.* **2005**, *127*, 6374. (k) Kubota, Y.; Takata, M.; Matsuda, R.; Kitaura, R.; Kitagawa, S.; Kato, K.; Sakata, M.; Kobayashi, T. *C. Angew. Chem.* **2005**, *44*, 920. (l) Chun, H.; Dybtsev, D. N.; Kim, H.; Kim, K. *Chem.–Eur. J.* **2005**, *11*, 3521. (m) Dybtsev, D. N.; Chun, H.; Yoon, S. H.; Kim, D.; Kim, K. *J. Am. Chem. Soc.* **2004**, *126*, 32. (n) Kaye, S. S.; Long, J. R. *J. Am. Chem. Soc.* **2005**, *127*, 6506. (o) Dinca, M.; Long, J. R. *J. Am. Chem. Soc.* **2005**, *127*, 9376. (p) Férey, G.; Latroche, M.; Serre, C.; Millange, F.; Loiseau, T.; Percheron-Guégan, A. *Chem. Commun.* **2003**, 2976. (q) Dubinin, M. M.; Astakhov, V. A. *Adv. Chem. Ser.* **1971**, *102*, 69.
- (3) Hydrothermal reaction of Zn(NO₃)₂·6H₂O (0.197 g, 0.66 mmol), H₂tbp (0.148 g, 0.66 mmol) with mixture solution of 13 mL of H₂O and 3 mL of ethylene glycol at 180 °C for 3 days generated uniform brown column crystals (0.082 g) of **1** in 42% yield, after filtering and washing by distilled water (3 × 30 mL), followed by ethanol (3 × 30 mL) and drying in air. IR (cm⁻¹): 3448 (br), 2994 (vs), 2974 (s), 1621 (vs), 1544 (vs), 1433 (s), 1417 (s), 1376 (vs), 1307 (s), 1514 (s), 1258 (m), 1188 (s), 1111 (s), 935 (s), 910 (m), 804 (m), 771 (vs), 743 (m), 714 (vs), 694 (s), 641 (m), 575 (s), 534 (m), 506 (s). PXRD of the bulk samples was in excellent agreement with the simulated PXRD pattern.
- (4) Crystal data of **1**: C₁₂H₁₂O₄Zn, $M = 285.59$ g/mol, trigonal, space group $R\bar{3}m$, $a = 28.863(4)$ Å, $c = 7.977(2)$ Å, $V = 5755.1(18)$ Å³, $Z = 18$, $F(000) = 2628$, $D_c = 1.483$ g cm⁻³, $\mu(\text{Mo K}\alpha) = 1.919$ mm⁻¹, 97 variables refined on F^2 with 1050 observed reflections collected at 293(2) K ($\theta_{\text{max}} = +25.97^\circ$) with $I \geq 2\sigma(I)$ yielding $R1 = 0.033$, $wR2 = 0.087$, $\text{GOF} = 1.047$.
- (5) Janiak, C. *J. Chem. Soc., Dalton Trans.* **2000**, 2885.
- (6) Spek, A. L. *PLATON, A Multipurpose Crystallographic Tool*; Utrecht University: Utrecht, The Netherlands, 2001.
- (7) TG experiment was carried out under N₂ at a heating rate of 5 °C/min.

JA057667B